Atmos. Meas. Tech. Discuss., 6, 9263–9295, 2013
www.atmos-meas-tech-discuss.net/6/9263/2013/
doi:10.5194/amtd-6-9263-2013

Atmospheric Measurement Techniques Discussions

Characterization and mitigation of water vapor effects in the measurement of ozone by chemiluminescence with nitric oxide

P. Boylan[1,*], **D. Helmig**[1], **and J.-H. Park**[1]

[1]Institute of Arctic and Alpine Research (INSTAAR), University of Colorado, Boulder, USA
[*]now at: Earth Observing Laboratory, NCAR, Boulder, CO, USA

Received: 4 September 2013 – Accepted: 7 October 2013 – Published: 29 October 2013

Correspondence to: D. Helmig (detlev.helmig@colorado.edu)

Published by Copernicus Publications on behalf of the European Geosciences Union.

Abstract

Laboratory experiments were conducted to investigate the effects of water vapor on the reaction of nitric oxide with ozone in a chemiluminescence instrument used for fast response and high sensitivity detection of atmospheric ozone. Water vapor was introduced into a constant level ozone standard and both ozone and water vapor signals were recorded at 10 Hz. The presence of water vapor was found to reduce, i.e. quench the ozone signal. A correction factor was determined to be $4.15 \pm 0.14 \times 10^{-3}$, which corresponds to a 4.15 % increase in the measured ozone signal per 10 mmol mol^{-1} co-sampled water vapor. An ozone-inert water vapor permeable membrane (Nafion dryer) was installed in the sampling line and was shown to remove the bulk of the water vapor mole fraction in the sample air. At water vapor mole fractions above 25 mmol mol^{-1}, the Nafion dryer removed over 75 % of the water vapor in the sample. This reduced the ozone signal correction from over 11 % to less than 2.5 %. The Nafion dryer was highly effective at reducing the fast fluctuations of the water vapor signal (more than 97 %) while leaving the ozone signal unaffected, which is a crucial improvement for minimizing the interference of water vapor fluxes on the ozone flux determination by the eddy covariance technique.

1 Introduction and background

Recent developments in instrumentation for ambient air ozone measurements have enabled direct observations of open ocean atmospheric ozone concentrations and fluxes. The measurement of ozone is based on the chemiluminescence reaction of ozone (O_3) and nitric oxide (NO) (Reaction R1), which emits light between 600 nm < λ < 2800 nm that is detected with a photomultiplier tube (PMT):

$$NO + O_3 \xrightarrow{k_1} NO_2^* + O_2 \qquad \text{(R1)}$$

AMTD
6, 9263–9295, 2013

$$NO_2^* \xrightarrow{k_2} NO_2 + h\nu \quad \text{(R2)}$$

$$NO_2^* + M \xrightarrow{k_3} NO_2 + M \quad \text{(R3)}$$

The excited nitrogen dioxide (NO_2) reaches equilibrium through photoemission (Reaction R2). NO_2^* can also react with a molecule through collisional energy transfer, reducing it to the ground state and effectively quenching the signal (Reaction R3). The chemiluminescence signal resulting from the reaction of nitric oxide and ozone is sensitive to several other atmospheric molecules such as H_2, CO_2, and H_2O (Matthews et al., 1977). An earlier study did not find an effect of water vapor at 75 % saturation when compared to 0 % saturation on the O_3-NO chemiluminescence reaction (Fontijn et al., 1970). Subsequently, Matthews et al. (1977) found that water vapor is more than ten times more effective at quenching the chemiluminescence signal than molecular hydrogen and more than three times more effective than carbon dioxide, which makes water the primary interferent of this ozone measurement under ambient air conditions. In contrast to the O_3-NO chemiluminescence measurement, instruments based on the reaction of ozone and ethylene reported an increase in ozone signal with water vapor (Kleindienst et al., 1993). This was determined to be due to a second compound being formed in the presence of water vapor that generates chemiluminescence.

Instead of correcting for the quenching effect of water vapor, some instruments were configured to supply a flow of water vapor to the reaction chamber to keep the effect of water vapor constant, complicating the operation of the system (Ridley and Grahek, 1990). Another proposed method to account for the quenching effect of water was to approximate the reduction in the ozone signal as a function of the water vapor mole fraction and apply a correction factor (Lenschow et al., 1981; Ridley et al., 1992):

$$O_3 = O_{3m}(1 + \alpha r) \quad (1)$$

where O_3 is the corrected ozone mole fraction, O_{3m} is the measured ozone volumetric mole fraction in nmol mol^{-1}, α is the correction factor, and r is the water vapor

AMTD
6, 9263–9295, 2013

mole fraction (expressed as the ratio of moles of water vapor to moles of dry air in mmol mol^{-1}, which is equivalent to parts per thousand). Lenschow et al. (1981) reported the α correction factor as $5 \times 10^{-3} \pm 1 \times 10^{-3}$ and the work of Ridley et al. (1992) further refined the value to $4.3 \times 10^{-3} \pm 0.3 \times 10^{-3}$. For example, for a typical equatorial region open ocean atmospheric water vapor mole fraction of 30 mmol mol^{-1} the correction accounts to 15 % when using the correction factor of 5×10^{-3}. A correction of this magnitude was applied by Williams et al. (2006) in their chemiluminescence measurement of ozone. Previous work has not detailed if and how much the correction factor is dependent on instrument configuration and operational conditions, or if this correction is universally applicable. Prior to the experiments described here, the correction factor had not been determined for our particular custom-built fast-response ozone instrument (FROI). Previous work with this instrument had therefore selected $\alpha = 5 \times 10^{-3}$ according to Lenschow et al. (1981), which resulted in up to a 25 % correction for determining the atmospheric ozone mole fraction (Lang, 2008; Bariteau et al., 2010; Helmig et al., 2012b).

A benefit of the fast response time and high sampling frequency of a chemiluminescence ozone instrument is the ability to define surface fluxes in combination with a sonic anemometer by the eddy covariance technique. Applying a correction to the ozone signal to account for the water vapor influences is particularly critical for these eddy covariance calculations as these are susceptible to interferences from the total atmospheric water vapor mole fraction and the water vapor flux. Our FROI has been deployed for ozone flux determination to locations vastly ranging in water vapor content, from the dry arctic to the equatorial ocean (Bariteau et al., 2010; Helmig et al., 2012a; Helmig et al., 2012b). Reynolds averaging of the corrected ozone signal in Eq. (1) and the vertical component of the wind vector results in the following equation for the water vapor corrected ozone flux:

$$F_{O_3} = \left(1 + \alpha \bar{r}\right) F_{O_{3m}} + \alpha \overline{O_{3m}} \overline{w' r'}, \quad (2)$$

AMTD
6, 9263–9295, 2013

where F_{O_3} is the corrected ozone flux, α is the correction factor, $\bar{r}$ is the mean water vapor mole fraction, $F_{O_{3m}}$ is the calculated ozone flux from the measured ozone signal, and $\overline{w'r'}$ is the average water vapor flux. There are three cases for the interaction between the water vapor flux and the ozone flux: (1) no water vapor flux – no correction for the ozone flux is needed; (2) downward water vapor flux and downward ozone flux – the uncorrected measured ozone fluxes are greater than actual ozone fluxes due to the effect of water vapor; and (3) upward water vapor flux and downward ozone flux – the uncorrected measured ozone fluxes are less than actual ozone fluxes due to the effect of water vapor fluctuations. The magnitude of ozone fluxes varies significantly based on surface properties. Relatively large ozone fluxes, up to $-0.4\,\mathrm{nmol\,mol^{-1}\,m\,s^{-1}}$, have been observed over vegetated land, such as over soybean fields (Wesely and Hicks, 2000) and over tropical forests (Cros et al., 2000). Much smaller ozone fluxes are observed over snow, ice, and water, typically ranging from -0.01 to $-0.08\,\mathrm{nmol\,mol^{-1}\,m\,s^{-1}}$ (Ganzeveld et al., 2009; Helmig et al., 2009, 2012a, b). Interestingly, upward ozone fluxes up to $0.1\,\mathrm{nmol\,mol^{-1}\,m\,s^{-1}}$ have been observed in subalpine forests during the winter (Zeller, 2000). To illustrate the sensitivity of the ozone flux to the water vapor flux, the relative correction to be applied to the ozone flux calculation as a function of the water vapor flux is illustrated in Fig. 1. For this simulation, typical oceanic values for ambient air water vapor and ozone mole fraction were chosen. The water vapor flux was varied between $\pm 4.5 \times 10^{-5}\,\mathrm{g\,kg^{-1}\,m\,s^{-1}}$ (Edwards, 2007), ozone was set at $40\,\mathrm{nmol\,mol^{-1}}$ and the water vapor content was $18\,\mathrm{mmol\,mol^{-1}}$ (Bariteau et al., 2010).

The green shaded regions illustrate conditions when the fluxes are in opposite directions. This results in a negative error of the measured ozone flux. Blue regions represent conditions where the ozone and water vapor fluxes are in the same direction, which results in a positive error of the measured ozone flux. For example, an ozone flux of $-0.05\,\mathrm{nmol\,mol^{-1}\,m\,s^{-1}}$ and water vapor flux of $0.05\,\mathrm{g\,kg^{-1}\,m\,s^{-1}}$ results in a corrected ozone flux of $-0.0445\,\mathrm{nmol\,mol^{-1}\,m\,s^{-1}}$, a difference of 11 %. If the water vapor flux is in the same direction as the ozone flux ($-0.05\,\mathrm{g\,kg^{-1}\,m\,s^{-1}}$) the corrected

AMTD
6, 9263–9295, 2013

flux is $-0.0645\,\mathrm{nmol\,mol^{-1}}$, a difference of 29 %. During several open ocean research cruises, Bariteau et al. (2010) calculated corrections of up to 25 % to the ozone flux due to the water vapor flux. The FROI measures the mole fraction of ozone relative to air with varying amounts of water vapor. When computing ozone fluxes in the presence of water vapor, density corrections must also be applied to the ozone flux (Webb et al., 1980). The dilution correction is similar to Eq. (1) with an α value of 1.61, which is the ratio of the molecular weight of dry air to the molecular weight of water vapor (Bariteau et al., 2010). Dilution corrections are applied before the water flux corrections. The density correction for ozone fluxes observed in the Gulf of Mexico was an additional 8 % on average (Bariteau et al., 2010). Applying a large correction to the ozone signal is undesirable as it leads to a greater uncertainty in the flux determination. An alternative is to selectively remove water from the sample. To achieve this goal a Nafion drying membrane has been implemented in both chemiluminescence and UV absorption ozone instruments (Wilson and Birks, 2006; Lang, 2008; Bariteau et al., 2010; Spicer et al., 2010; Helmig et al., 2012b). The hydrophilic properties of the membrane make it permeable to water vapor without affecting the ozone signal (Wilson and Birks, 2006). The drying performance of the Nafion dryer is not uniform and depends on the type of Nafion dryer, length, sample and drying flows, and drying gas used. The amount of water vapor removed by the Nafion dryer has been found to vary from ∼ 25 % to over 70 % (Lang, 2008; Bariteau et al., 2010; Spicer et al., 2010). Analytical tests have shown that ozone is not removed by the Nafion membrane (Wilson and Birks, 2006; Spicer et al., 2010).

Preliminary observations from our system indicated that the use of a Nafion drying system diminished the high frequency water vapor fluctuations, which reduced the water vapor flux by 98 % and eliminated the need for density and quenching corrections (Bariteau et al., 2010). The effects of the Nafion dryer on high frequency ozone signals were not investigated in detail in that study; however, Bariteau et al. (2010) reported no apparent reductions in the ozone flux. In this paper, the effects of water vapor and the installation of a Nafion drying system on our chemiluminescence ozone instrument

AMTD
6, 9263–9295, 2013

were studied in more depth, with a critical examination of the applicability of the correction factors determined in the earlier work of Lenschow et al. (1981) and Ridley et al. (1992).

2 Instrumentation and methodology

Ozone was measured by a custom-built FROI with a precision sufficient to resolve small changes in ozone mole fractions at a high temporal resolution. The FROI has a sensitivity of ~ 2000 counts s^{-1} $ppbv^{-1}$ and a background noise of 900 counts s^{-1}. Details and a schematic of the FROI have been published by Bariteau et al. (2010) (see Fig. 1 in this reference for a schematic of the FROI). Sample air was pulled through a Teflon® (PFA, perfluoroalkoxy copolymer) line controlled to 1.5 L min^{-1} by a mass flow controller (MFC). All ozone sample tubing was 0.64 cm outer diameter Teflon® tubing. Nitric oxide reactant gas flowed through stainless steel tubing and was controlled at 3 mL min^{-1}. The sample and NO were mixed in a 44 cm^3 gold-plated reaction chamber. The reaction chamber temperature was maintained at 30 °C by a heater and temperature controller. An integrated PMT housing Peltier cooler maintained the PMT temperature at −30 °C (Hamamatsu, Model C10372, Japan), essential to reach low noise and high sensitivity levels. The reaction chamber pressure was controlled to 18 Torr by a pressure controller (UPC 1300, Coastal Instruments) downstream of the reaction chamber, which asserted that the instrument response was insensitive to fluctuations in the sample delivery flow rate. Photons were counted by a PMT (Hamamatsu Photonics K. K., Shizuoka, Japan) with a cutoff filter (RG-610, Newport Industrial Glass, Stanton, CA) removing radiation with wavelengths less than 600 nm. The FROI was calibrated against a commercial UV absorption instrument (Model TEI 49i, Thermo Scientific, Franklyn, MA, USA). This UV-instrument was referenced against the ozone standard at the Global Monitoring Division (GMD), National Oceanic and Atmospheric Administration (NOAA), Boulder, Colorado.

AMTD
6, 9263–9295, 2013

A detailed schematic of the experimental setup is shown in Fig. 2. Water vapor measurements were achieved with a high precision closed path infrared hygrometer (LI-COR LI-7000, LI-COR Inc., Lincoln, NE, USA). The sample flow for the LI-COR was controlled at 1.5 $L\,min^{-1}$ using a MFC. The LI-7000 recorded water vapor data as $mmol\,mol^{-1}$. A water removal system was designed around a 2.44 m Nafion dryer (MD-110-96F, Perma Pure LLC, Toms River, NJ, USA). The pressure in the dryer outer annual space was maintained at a lower pressure to prevent the collapse of the inner membrane. The sample flow and dryer flow ran in opposite directions. The Nafion dryer system included a rotameter and needle valve for regulating the dryer flow, a drying unit filled with $CaSO_4$ (W. A. Hammond Drierite Co. LTD, OH, USA), and a tank of breathing air. The water vapor content in the breathing air tank was less than 0.03 $mmol\,mol^{-1}$. The flow of the drying air in the Nafion system was maintained between two and three times the sample flow. The sample flow passing through the Nafion dryer was 3.0 $L\,min^{-1}$ (FROI + LI-COR).

A tank of breathing air supplied ozone-free air to the TEI 49i which was used for generating ozone. Ozone was produced by setting the TEI 49i generator to a constant ozone output level. The flow rate was held constant at 1.0 $L\,min^{-1}$ by MFC 4. The ozone output was set to different levels by adjusting the intensity of the UV light source inside the TEI 49i. The resulting ozone output was checked with the TEI 49i regularly and found to be stable based on the comparison of measured ozone levels prior to and after experiments that used a particular ozone output level. The ozone generation process was kept separate from the humidifying process to ensure constant ozone production regardless of water vapor content. The ability to regulate the water vapor content in the air was accomplished by using a "zero-air" generator and a Drierite column and by changing the split ratio and balancing the total flow between MFC 1 and MFC 2. The combined flow through these two MFC was held constant at $\sim 9\,L\,min^{-1}$. The introduction of water vapor in the sample air was accomplished by operating a Nafion dryer in reverse mode: liquid water was pumped through the inner tubing while dry air from MFC 2 flowed in the outer tube. Maximum water vapor mole

AMTD
6, 9263–9295, 2013

fractions were achieved when MFC 2 was set to 9.0 L min^{-1} and MFC 1 was closed. MFC 3 was set to 8.0 L min^{-1}, leaving an excess flow to the vent of 1 L min^{-1}. This configuration allowed for controlling a continuous range of water vapor mole fractions between < 0.1 and 28 mmol mol^{-1}.

This study used 4 ozone (0, 30, 60 and 100 nmol mol^{-1}) and 6 water vapor mole fraction levels (< 0.1, 6, 12, 18, 23 and 27 mmol mol^{-1}) to mimic a range of atmospheric conditions. These levels were tested with and without the Nafion dryer installed, yielding 48 sampling periods. Ozone was set to one of the 4 levels, then the water vapor was varied across each of the 6 water vapor levels. Water vapor levels were varied both from high to low and low to high. Each sampling period was run for at least 15 min after both the water vapor and ozone signals equilibrated to new conditions. All data were sampled and recorded at 10 Hz. Data from each sampling period were reduced to 15 min for consistency between sampling periods.

In our experimental configuration MFCs 3 and 5 were subjected to sample air with varying water vapor mole fraction. The changing humidity in the sample flow bears the potential to effect the ability of the MFC to maintain a constant flow rate, resulting possibly in a difference between the MFC set point flow and the actual flow rate. This effect could potentially bias the results from these experiments, in that changes in flow rate and dilution ratio could mistakenly be interpreted as a change in the FROI detection sensitivity. It has previously been noted that the effect of water vapor on MFC flow rates is nonlinear, making the scaling relations of the MFC particularly challenging (Wang, 2012; B. Darby, Coastal Instruments, personal communication, 5 March 2013). In order to investigate the effect of water vapor on MFC flow rates, MFC 3, a Tylan FC-2900 with a flow range of 0–30 L min^{-1} was subjected to variable humidity levels while the set-point flow rate was kept constant at 8 L min^{-1}. Reference flow rates were determined with a bubble meter, corrected for temperature and pressure to yield mass flow rates, and then compared with the set point flow rates. For dry air, at a MFC set point of 8 L min^{-1}, the MFC displayed flow was 7.98 L min^{-1} while the bubble meter calibration gave 8.12 L min^{-1}. Water vapor was then introduced into the sample flow at 5 levels be-

AMTD
6, 9263–9295, 2013

tween 4 and 26 mmol mol^{-1} and 20 bubble meter flow readings were recorded at each level (Fig. A1). At all tested water vapor levels at and above 0.4 mmol mol^{-1}, while the MFC reported that the flow remained constant at 7.98 L min^{-1}, the flow rate determined with the bubble meter was 7.93 L min^{-1}, a drop of 2.3 %. A one-way analysis of variance (ANOVA) found this difference to be statistically significant at the $p < 0.05$ level, $F(5, 114) = 15.9$, $p = 1.35 \times 10^{-9}$. Furthermore, post hoc comparison using the Tukey test (Hsu, 1996) indicated that the mean bubble meter reported flow for the dry air was significantly different than the individual results at each of the humidified air levels. The same calculations revealed that there was no significant difference between any of the tested humidified air levels.

The same analysis was conducted on MFC 5, a Tylan FC-260 with a range of 0–5 L min^{-1}, yielding similar results, i.e. a drop of 2.6 % (Fig. A2) and statistical significance. Taken together, these results indicate that the MFCs exhibit a significant drop in flow between dry and humidified air (2.3–2.6 %), but that flows were not affected over a wide range of humidity once a threshold value (in our case ~ 4 mmol mol^{-1}) has been exceeded. For this manuscript, flow rates from experiments with dry air were corrected for this bias, but no further corrections were applied for experiments conducted at humilities > 4 mmol mol^{-1}. It's noteworthy that in the experimental setup used here, the bias of MFC 3 was attenuated somewhat as the resulting ozone mole fraction delivered depends on the flow ratio of MFC 4/(MFC 3 + MFC 4). Furthermore, the MFC biases of MFC 3 and MFC 5 cancel out each other to a significant degree (~ 75 %). When MFC 3 experienced a drop in flow going from dry to moist air, the ozone mole fraction in the ozone standard sample slightly increased from the change in the dilution ratio as the output from the 49i remained constant. The response of MFC 5 in this transition was a slight reduction of the flow provided to the FROI, causing a reduction in the FROI response. The net effect of the MFC 3 and MFC 5 flow changes on the ozone signal was calculated as 0.54 %.

Experiments under ambient conditions were conducted to test the effect of the Nafion dryer on high frequency fluctuations of the water vapor signal. This experiment

AMTD
6, 9263–9295, 2013

took place behind the NOAA David Skaggs Research Center in Boulder, CO in October 2008. The footprint of the sampling location consisted of a small parking lot surrounded by surface vegetation. The same FROI and Nafion drying system setup were used in this experimental setup. Water vapor was measured by two LI-7500 (LI-COR Inc., Lincoln, NE, USA) hygrometers. These hygrometers were converted to closed path instruments by inserting the calibration tube between the sapphire-glass windows. The FROI and the two LI-CORs were housed in a container for weather protection. Ambient air was drawn through a 23 m sampling line with an inlet located at 4 m height on a meteorological tower. A Teflon® membrane filter (5 µm, Millipore, Billerica, MA, USA) was used during ambient air measurements to prevent contamination of the tubing due to air pollutants. The air passed through one LI-COR, then through the Nafion dryer followed by the other LI-COR, before sampling by the FROI. Prior to the experiment, an inter-comparison of both LI-CORs was conducted to determine the offset between the instruments. The ambient air ozone mole fraction was $\sim 39\,\mathrm{nmol\,mol^{-1}}$ and the water vapor mole fraction varied between 4 and 6 $\mathrm{mmol\,mol^{-1}}$.

3 Results and discussion

3.1 Effects of water vapor on the chemiluminescence ozone signal

The water vapor mole fraction was varied across different ozone levels in order to determine the appropriate correction factor, α, for this instrument and to evaluate how the correction factor compares with previously reported results for other instruments. To determine the correction factor, a re-write of Eq. (1) is used, shown as:

$$O_{3,0} = O_{3,r}(1 + \alpha r) \quad (3)$$

where $O_{3,0}$ is the ozone signal in counts s^{-1}, when the water vapor mole fraction is $< 0.1\,\mathrm{mmol\,mol^{-1}}$, and $O_{3,r}$ is the ozone signal at a water vapor mole fraction r. At

AMTD
6, 9263–9295, 2013

each ozone level, the correction factor was calculated at each water vapor level with pairwise combinations of $O_{3,0}$ and $O_{3,r}$. As seen by arranging Eq. (3), the slope of the linear regression analysis of the ratio $O_{3,0}/O_{3,r}$ and the water vapor mole fraction corresponds to the correction factor, shown in Fig. 3. A consistent pattern was seen when water vapor was introduced to ozone-enriched air; an increase of water vapor caused a decrease of the ozone signal. Direct observations from this experiment showing the average ozone signal loss for each average water vapor level are presented in Table A1, the summary of these results are shown in Fig. 3. At high water vapor mole fractions the ozone signal had a negative bias of over 11 %.

The average correction factor based on the results from Fig. 3 gave a mean value for α of 4.15×10^{-3} with a 95 % confidence interval of 0.14×10^{-3}. This result is within the range given by Lenschow et al. (1981) ($5 \times 10^{-3} \pm 1 \times 10^{-3}$) and Ridley et al. (1992) ($4.3 \times 10^{-3} \pm 0.3 \times 10^{-3}$). Our instrument was operated at 10 Hz; Lenschow et al. (1981) used a sampling frequency of 20 Hz and Ridley et al. (1992) sampled at 12 Hz. Despite their reaction chamber being half the size of ours at 17 cm^3 with a sensitivity of 2000 counts s^{-1} $ppbv^{-1}$ it yielded a similar response to our instrument. The important conclusion from these comparisons is that, despite these differences in the instrument configuration, the correction factors determined by these three studies all agree within the margin of error provided by each study.

3.2 The removal of water vapor with a Nafion drying system

The Nafion dryer was installed in the sample line (Fig. 2) upstream of the FROI and LI-COR. Switching valves allowed for the flow to pass through or to bypass the Nafion dryer. The experiment from the previous section was repeated with the addition of the Nafion drying system. A time series of the water vapor mole fraction recordings in the sample flow as it bypassed the Nafion dryer and flowed through the Nafion dryer is shown in Fig. 4. Each sampling period started with the flow bypassing the Nafion dryer to record the amount of water vapor in the sample. In Fig. 4 the flow bypassed the Nafion dryer for the first 2 min, during that time the LI-COR recorded 12.2 $mmol\,mol^{-1}$.

AMTD
6, 9263–9295, 2013

After two minutes the flow was switched to the Nafion dryer and the water vapor mole fraction dropped below 5 mmol mol^{-1}. It took between 7 and 12 min for the water vapor to equilibrate at 4.6 mmol mol^{-1}. The flow was then switched back to bypass the Nafion dryer to ensure reproducible water vapor conditions throughout the experiment. This behavior was repeatable during operation of the Nafion drying system over a period of several days.

The amount of water vapor removed from the sample air under the range of applied conditions is shown in Fig. 5. The drying efficiency was consistent across ozone levels. The Nafion dryer removed 50 % of the water at the lower water vapor mole fractions. This is a higher rate than what was reported in a previous study with this Nafion setup where a 28 % removal rate of water vapor through the Nafion system using ambient air with a water vapor mole fraction of ~ 5 mmol mol^{-1} was observed (Lang, 2008; Bariteau et al., 2010). Under the laboratory conditions tested here, the Nafion dryer became more efficient at higher water vapor mole fractions, removing up to 78 % of the water vapor in the sample air at the highest humidity conditions that could be tested.

Additional tests were performed to determine the optimum configuration for the Nafion drying system. During the above described experiments, the sample flow through the Nafion drying system was 3.0 L min^{-1} and the drying flow was set at 9.0 L min^{-1}. The drying flow was lowered to 6.0 L min^{-1} to investigate the relationship between dryer flow and water vapor removal. The comparison between these two dryer flows revealed a statistical difference in the amount of water vapor removed. The 9.0 L min^{-1} drying flow removed 77.4 % of the water vapor while the lower drying flow of 6.0 L min^{-1} removed 75.0 %. There was not a statistical difference in the ozone signals between the high drying flow rate and low drying flow rate.

A comparison was also done between the 2.44 m-long (used for the entirety of this experiment) and a 1.22 m-long dryer under similar conditions. At a water vapor mole fraction of 26 mmol mol^{-1}, the 2.44 m dryer removed 78 % while the 1.22 m dryer removed 71 % of the supplied amount of water vapor. Obviously, the removal rate of water vapor does not scale linearly with the drying gas flow rate and the length of the

AMTD
6, 9263–9295, 2013

Nafion dryer. It is important to note that drying efficiency is variable and dependent on multiple operational conditions that do not scale linearly.

3.3 Effect of the Nafion dryer on the ozone signal

First, we tested if there was a loss of ozone as it passed through the Nafion dryer by comparing three configurations: (1) a control case without the Nafion dryer installed, (2) Nafion dryer installed with drying flow rate of 0.0 L min^{-1}, and (3) Nafion dryer installed with drying flow rate of 9.0 L min^{-1}. All three cases used a dry sample flow containing < 0.1 mmol mol^{-1} water vapor and 60 nmol mol^{-1} ozone. The mean ozone signals measured for these three setups were basically the same, varying by 40 counts s^{-1} (0.03 % of 130 000 counts s^{-1}), which is within the sampling noise of the instrument and not statistically different. This confirmed previous research that reported that ozone passes through the Nafion dryer without any noticeable losses (Wilson and Birks, 2006; Spicer et al., 2010).

After confirming that there is no ozone loss in the Nafion dryer, we investigated how much of the ozone signal loss seen in the experiments described above is restored by passing a humidified sample flow through the dryer. When using a Nafion drying system, there are two effects that need to be considered: (1) an enrichment (i.e. increase in mole fraction) of ozone resulting from the removal of water molecules and (2) the reduction of the quenching effect occurring in the reaction chamber.

The Nafion drying system operates on the principle of removing molecules of water vapor from the sample line by permeation through a semi-permeable membrane. Since this causes a reduction of the total amount of molecules while the number of ozone molecules remains constant, the use of the dryer results in an enrichment of ozone, i.e. an increase in the ozone mole fraction and the signal from the FROI. The enrichment effect is expected to be equal to the fraction of water vapor molecules removed by the Nafion dryer. In the previous section it was shown, for instance, that at a water vapor mole fractions of ~ 25 mmol mol^{-1}, the Nafion dryer removed ~ 77 % of the water vapor, equivalent to ~ 20 mmol mol^{-1} (or 20 parts per thousand = 2 %). This

AMTD
6, 9263–9295, 2013

enrichment would consequently cause an increase in the FROI signal of 2 %. Figure 6 displays the inferred ozone enrichment as a function of the water vapor content, as measured upstream of the Nafion dryer, ranging from 0.3–2 % under the water vapor mole fractions applied here.

The ozone signal that is restored when using the Nafion dryer was determined by comparing results from three different cases. Case 1 is the sample flow containing 30 nmol mol^{-1} of ozone in dry air, < 0.1 mmol mol^{-1} of water vapor, without the sample passing through the Nafion dryer. Case 2 is a humidified sample containing 30 nmol mol^{-1} of ozone, a water vapor mole fraction of 6.04 mmol mol^{-1}, without passing through the Nafion dryer. Case 3 is for a sample flow with the Nafion dryer installed, containing 30 nmol mol^{-1} of ozone, 26.5 mmol mol^{-1} of water vapor upstream of the Nafion dryer and 6.04 mmol mol^{-1} of water vapor downstream of the Nafion dryer. In Cases 2 and 3, the amount of water vapor entering the FROI reaction chamber is very similar, at ∼ 6 mmol mol^{-1}. In theory, the ozone signal from Case 2 should be equal to the ozone signal from Case 1 after correcting for the quenching effect, and Case 3 should agree to Case 1 after correcting for the enrichment and quenching.

For Case 1, the FROI signal was 60 645 counts s^{-1} (Table 1). For Case 2, the corrected ozone signal was determined from the measured 59 135 counts s^{-1} by using Eq. (4), $\alpha = 4.15 \times 10^{-3}$, and $r = 6.04$ mmol mol^{-1} of water vapor. This yields a corrected ozone signal of 60 617 counts s^{-1}. The ozone signal for Case 3 required corrections for both enrichment and quenching. The difference in water vapor mole fractions upstream and downstream of the Nafion dryer was 20.1 mmol mol^{-1} of water vapor, which corresponded to 2.01 % of the total molecules in the sample flow being removed by the Nafion dryer. The measured ozone signal was 60 267 counts s^{-1} corresponding to an ozone signal of 59 079 counts s^{-1} after this correction. In order to account for the quenching effect, Eq. (4) was applied, with O_{3m} = 59 079 counts s^{-1}, $\alpha = 4.15 \times 10^{-3}$, and $r = 6.4$ mmol mol^{-1} of water vapor. This calculation resulted in a corrected ozone signal of 60 648 counts s^{-1}.

AMTD
6, 9263–9295, 2013

With these considerations, the three cases gave close agreement, with the difference between the three cases of less than 32 counts s^{-1} (or 0.02 nmol mol^{-1} of ozone), which is well within the precision of the FROI. This consistency confirms the correctness of the determined quenching effect, developed correction algorithms, and the efficiency of the Nafion dryer in mitigating the quenching effects in the FROI ozone detection.

3.4 Reduction of atmospheric water vapor high frequency signals

The high sampling frequency of the FROI and LI-COR allowed for the investigation of high frequency behavior of the ozone and water signal with use of the Nafion dryer, specifically the reduction of water vapor fluctuations that determine the water vapor flux in Eq. (3). The following analyses are based on the experiments conducted on the mesa behind the NOAA-ESRL building.

The water vapor power spectrum distributions with and without the Nafion dryer shown in Fig. 7a illustrate that the Nafion dryer was very efficient in damping the high frequency water vapor signal. The water vapor spectrum obtained without the Nafion dryer has both low and high frequency contributions. White noise was seen at frequencies higher than 2 Hz. The water vapor spectrum with the Nafion dryer installed has its primary contribution in the lower frequency range and a reduction of the higher frequencies when compared to the water vapor signal without the Nafion dryer. The ratio of the integrals of the power spectra showed a 77 % reduction of water vapor mole fraction, which confirmed the amount of water vapor removed as seen at the highest water vapor levels in Fig. 5.

The frequency response spectrum in Fig. 7c shows the coherency between the water vapor with and without a Nafion dryer. The coherency is the ratio of the cospectrum between the two water vapor signals and the square root of the product of the power spectra. A coherency value of 1 is representative of a high correlation between two signals at a given frequency. The water vapor signals have high coherency between 10^{-3} and 10^{-2} Hz, a decrease between 10^{-2} and 10^{-1} Hz, and display low coherence

AMTD
6, 9263–9295, 2013

above 0.1 Hz. These results clearly illustrate that the Nafion dryer is very effective at reducing the high frequency contributions of the water vapor measurements. By using the integral of the cospectrum we found that the water vapor flux was reduced by 97 %.

It is imperative that the attenuation of fast fluctuations as observed in the water vapor signal is not seen in the ozone signal, as this would alter the ozone flux calculation. Figure 7b shows the power spectra of the ozone signal with and without the Nafion dryer installed in the sampling flow path. The ozone signal has a relatively large contribution from lower frequencies in the < 0.1 Hz range. The inertial subrange is between 0.1 and 0.7 Hz. White noise is seen at frequencies higher than 0.7 Hz. The spectral components of the ozone signal remained unchanged when using the Nafion dryer, which confirms earlier results presented in this manuscript that there is not an attenuation of the ozone signal by the Nafion dryer. A slight increase of the signal is apparent in white noise frequencies greater than 0.7 Hz. This increase was observed in other time periods examined and can be explained by the additional tubing required of the Nafion dryer. These results give confidence in the ability to use a Nafion drying system when measuring ozone surface fluxes.

3.5 Inlet filter test

In order to prevent contamination of the sampling line from salt water sea spray, or other particulate matter, it has been a standard operating procedure to direct the sample air through a Teflon membrane inline sampling filter. Filters used in our field measurements are conditioned prior to use by purging $\sim 300\,\mathrm{nmol\,mol^{-1}}$ of ozone through the filter for $\sim 15\,\mathrm{h}$ at a flow rate of $4\,\mathrm{L\,min^{-1}}$. Filters are typically changed daily on oceanic research cruises in order to minimize the buildup of particulate matter on the filter. The effects of the Teflon filter on both the ozone and water vapor signal were investigated in the controlled laboratory setting. The filter was inserted into the setup directly downstream from the mixing of air from MFCs 3 and 4. Ozone and water vapor were held constant at $\sim 100\,\mathrm{nmol\,mol^{-1}}$ and $26\,\mathrm{mmol\,mol^{-1}}$ respectively. The difference in ozone and water vapor mole fractions with and without the filter were within the sampling noise of the

AMTD
6, 9263–9295, 2013

instrument. There was no significant difference in absolute water vapor or ozone mole fractions and fast fluctuations with and without the filter installed.

4 Summary and conclusions

This investigation confirmed previously reported signal loss in an O_3-NO chemiluminescence instrument from the presence of atmospheric water vapor. The quenching effect of water vapor resulted in up to an 11 % loss in the ozone signal as measured by the FROI. A correction factor, α, according to Eq. (1), was calculated to be 4.15×10^{-3} for our system used, which is of similar magnitude as results from previous researchers. We also demonstrated the effectiveness of a Nafion drying system to reduce the quenching effect of water vapor on the chemiluminescence signal. This was accomplished by a series of laboratory and outside ambient air experiments. The installation of a Nafion drying system significantly reduced the amount of water vapor in the sample air. The fraction of water vapor removed by the dryer was non-linear, increasing from ~ 50 % at 6 mmol mol^{-1} water vapor to over 70 % above 18 mmol mol^{-1} of water vapor. The drying efficiency was found to depend on operating conditions of the dryer, increasing with dryer length and drying flow rate. The removal of water vapor molecules by the Nafion dryer results in an ozone enrichment upwards of 2 %. Most importantly, the Nafion dryer was found to be effective at attenuating the fast fluctuations of the water vapor signal. The ozone mean concentration and ozone fast fluctuations were not affected by the Nafion dryer. Consequently, the Nafion dryer is an efficient means for eliminating the interference from the water vapor flux in the eddy covariance ozone flux measurement.

Acknowledgements. We thank K. Lang, and L. Bariteau, NOAA ESRL, Boulder CO, for providing data for the ambient water vapor and ozone flux experiments, and C. Fairall, also at NOAA ESRL, for helpful discussions.

AMTD
6, 9263–9295, 2013

References

Bariteau, L., Helmig, D., Fairall, C. W., Hare, J. E., Hueber, J., and Lang, E. K.: Determination of oceanic ozone deposition by ship-borne eddy covariance flux measurements, Atmos. Meas. Tech., 3, 441–455, doi:10.5194/amt-3-441-2010, 2010.

Cros, B., Delon, C., Affre, C., Marion, T., Druilhet, A., Perros, P. E., and Lopez, A.: Sources and sinks of ozone in savanna and forest areas during EXPRESSO: airborne turbulent flux measurements, J. Geophys. Res. Atmos., 105, 29347–29358, doi:10.1029/2000jd900451, 2000.

Edwards, J. M.: Oceanic latent heat fluxes: consistency with the atmospheric hydrological and energy cycles and general circulation modeling, J. Geophys. Res. Atmos., 112, D06115, doi:10.1029/2006jd007324, 2007.

Fontijn, A., Sabadell, A. J., and Ronco, R. J.: Homogeneous chemiluminescence measurement of nitric oxide with ozone – implications for continuous selective monitoring of gaseous air pollutants, Anal. Chem., 42, 575–579, doi:10.1021/ac60288a034, 1970.

Ganzeveld, L., Helmig, D., Fairall, C. W., Hare, J., and Pozzer, A.: Atmosphere-ocean ozone exchange: a global modeling study of biogeochemical, atmospheric, and waterside turbulence dependencies, Global Biogeochem. Cy., 23, GB4021, doi:10.1029/2008gb003301, 2009.

Helmig, D., Cohen, L. D., Bocquet, F., Oltmans, S., Grachev, A., and Neff, W.: Spring and summertime diurnal surface ozone fluxes over the polar snow at Summit, Greenland, Geophys. Res. Lett., 36, L08809, doi:10.1029/2008gl036549, 2009.

Helmig, D., Boylan, P., Johnson, B., Oltmans, S., Fairall, C. W., Staebler, R., Weinheimer, A., Orlando, J., Knapp, D., Montzka, D., Flocke, F., Freiß, U., Sihler, H., and Shepson, P.: Ozone dynamics and snow–atmosphere exchanges during ozone depletion events at Barrow, Alaska, J. Geophys. Res. Atmos., 117, D20303, doi:10.1029/2012JD017531, 2012a.

Helmig, D., Lang, E. K., Bariteau, L., Boylan, P., Fairall, C. W., Ganzeveld, L., Hare, J. E., Hueber, J., and Pallandt, M.: Atmosphere–ocean ozone fluxes during the TexAQS 2006, STRATUS 2006, GOMECC 2007, GasEx 2008, and AMMA 2008 cruises, J. Geophys. Res. Atmos., 117, D04305, doi:10.1029/2011jd015955, 2012b.

Hsu, J.: Multiple Comparisons: Theory and Methods, Chapman and Hall/CRC, Boca Raton, USA, 1996.

AMTD
6, 9263–9295, 2013

Ibrom, A., Dellwik, E., Larsen, S. E., and Pilegaard, K.: On the use of the Webb–Pearman–Leuning theory for closed-path eddy correlation measurements, Tellus B, 59, 937–946, doi:10.1111/j.1600-0889.2007.00311.x, 2007.

Kleindienst, T. E., Hudgens, E. E., Smith, D. F., McElroy, F. F., and Bufalini, J. J.: Comparison of chemiluminescence and ultraviolet ozone monitor responses in the presence of humidity and photochemical pollutants, J. Air Waste Manage., 43, 213–222, 1993.

Lang, K.: Ozone flux measurements during the Gulf of Mexico and East Coast Carbon Cruise 2007 (GOMECC), M.S. thesis, University of Potsdam, Potsdam, 88 pp., 2008.

Lenschow, D. H., Pearson, R., and Stankov, B. B.: Estimating the ozone budget in the boundary-layer by use of aircraft measurements of ozone eddy flux and mean concentration, J. Geophys. Res., 86, 7291–7297, doi:10.1029/JC086iC08p07291, 1981.

Matthews, R. D., Sawyer, R. F., and Schefer, R. W.: Interferences in chemiluminescence measurement of NO and NO_2 emissions from combustion systems, Environ. Sci. Technol., 11, 1092–1096, doi:10.1021/es60135a005, 1977.

Ridley, B. A. and Grahek, F. E.: A small, low flow, high-sensitivity reaction vessel for no chemiluminescence detectors, J. Atmos. Ocean. Tech., 7, 307–311, 1990.

Ridley, B. A., Grahek, F. E., and Walega, J. G.: A small, high-sensitivity, medium-response ozone detector suitable for measurements from light aircraft, J. Atmos. Ocean. Tech., 9, 142–148, 1992.

Spicer, C. W., Joseph, D. W., and Ollison, W. M.: A re-examination of ambient air ozone monitor interferences, J. Air Waste Manage., 60, 1353–1364, doi:10.3155/1047-3289.60.11.1353, 2010.

Wang, C.: Thermal Mass Flow Controller Scaling Relations, in: Measurement Science Conference, 22–23 March 2012, Anaheim, CA, 2012.

Webb, E. K., Pearman, G. I., and Leuning, R.: Correction of flux measurements for density effects due to heat and water-vapor transfer, Q. J. Roy. Meteor. Soc., 106, 85–100, doi:10.1002/qj.49710644707, 1980.

Wesely, M. L. and Hicks, B. B.: A review of the current status of knowledge on dry deposition, Atmos. Environ., 34, 2261–2282, 2000.

Williams, E. J., Fehsenfeld, F. C., Jobson, B. T, Kuster, W. C., Goldan, P. D., Stutz, J., and McCleanny, W. A.: Comparison of ultraviolet absorbance, chemiluminescence, and DOAS instruments for ambient ozone monitoring, Environ. Sci. Technol., 40, 5755–5762, doi:10.1021/es0523542, 2006.

AMTD
6, 9263–9295, 2013

Wilson, K. L. and Birks, J. W.: Mechanism and elimination of a water vapor interference in the measurement of ozone by UV absorbance, Environ. Sci. Technol., 40, 6361–6367, doi:10.1021/es052590c, 2006.

Zeller, K.: Wintertime ozone fluxes and profiles above a subalpine spruce-fir forest, J. Appl. Meteorol., 39, 92–101, 2000.

AMTD

6, 9263–9295, 2013

Table 1. Comparison of measured ozone signals (mean of 15 min data) at 30 nmol mol^{-1} (in counts s^{-1}) for Cases 1, 2 and 3, before and after applying each correction term.

Water Vapor Mole Fraction	Case 1 < 0.1 mmol mol^{-1} No Nafion Dryer	Case 2 6.04 mmol mol^{-1} No Nafion Dryer	Case 3 26.5 mmol mol^{-1} Nafion Installed
Measured Counts	60 645[a]	59 135	60 267
Corrected for Enrichment	N/A[b]	N/A	59 079
Corrected for Quenching	N/A	60 617	60 648

[a] Calculated from a raw count of 60 975 after correcting for the dry air flow biases of MFC 3 and MFC 5.
[b] Not applicable.

AMTD
6, 9263–9295, 2013

Table A1. Averaged loss of ozone signal at the 3 different ozone levels tested (30, 60, and 100 ppbv).

H_2O	Ozone signal loss ± 95 % confidence interval
6.2 ‰	2.5 ± 0.2 %
12.0 ‰	4.7 ± 0.4 %
17.9 ‰	7.1 ± 0.7 %
23.0 ‰	9.2 ± 0.6 %
27.1 ‰	11.2 ± 0.9 %

AMTD
6, 9263–9295, 2013

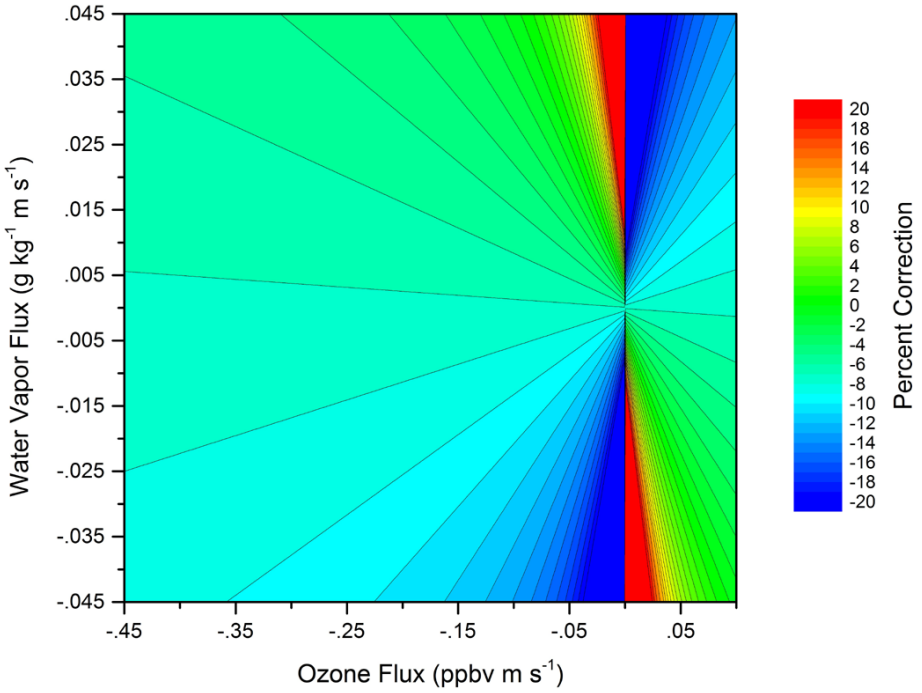

Fig. 1. Isopleths of the correction to be applied to the measured ozone flux as a function of water vapor flux. When the ozone fluxes and water vapor fluxes are in the same direction, the measured ozone flux has a positive error, as seen in the negative correction factor to be applied for quadrants 1 and 3. When the ozone flux and water vapor flux are in opposite directions, there is a negative error, requiring a positive correction to the measured ozone flux, as seen in quadrants 2 and 4.

AMTD
6, 9263–9295, 2013

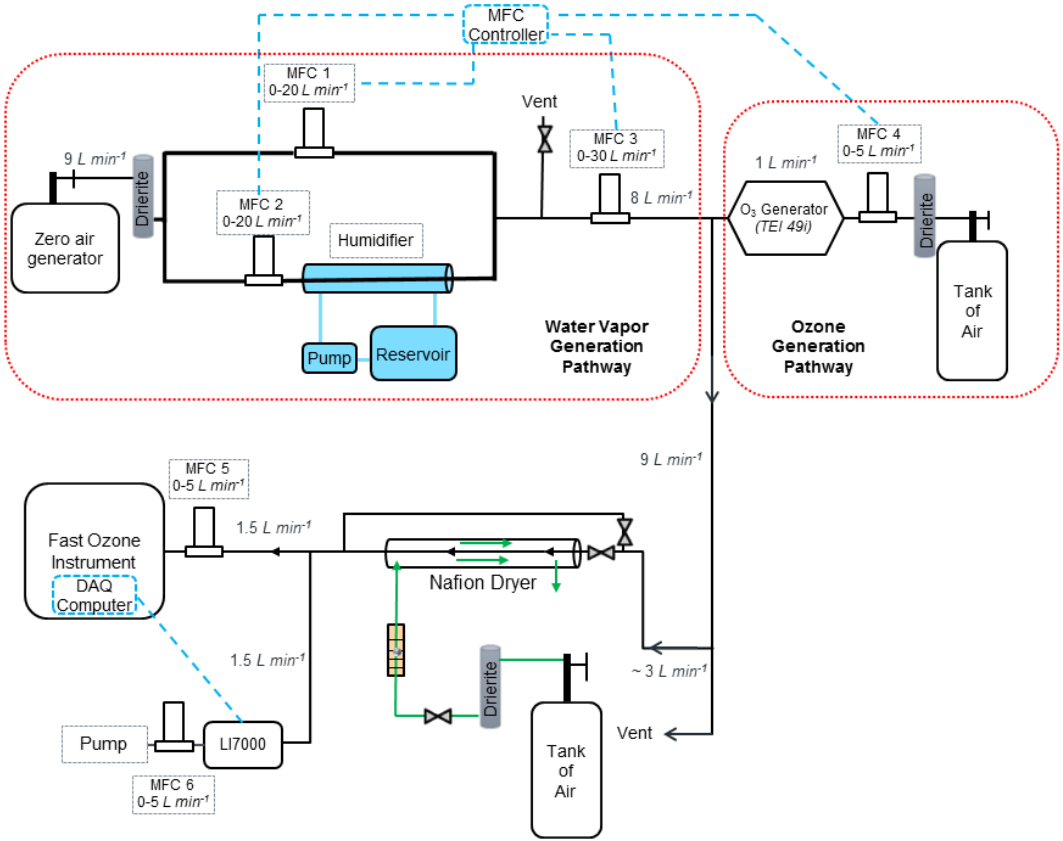

AMTD
6, 9263–9295, 2013

Characterization and mitigation of water vapor effects

P. Boylan et al.

Fig. 2. Schematic of the laboratory setup. The red box in the upper-left of the figure shows where the sample air was humidified. Ambient air was scrubbed through a zero-air generator and run through a drying agent to remove any excess water vapor. The flow was varied through mass flow controller (MFC) 1 to produce dry air and MFC 2 to produce humid air. The humidifier was a Nafion membrane containing liquid water in the inner tube and the sample flow through the outer shell. Excess flow was released through the vent with a flow restrictor. MFC 3 controlled the flow to 8 L min^{-1}. This air was mixed with ozone-enriched air from the TEI 49i ozone generator (red box in upper-right of figure). Sample air was provided from a tank of dry breathing air. The flow through the ozone generator was controlled to 1 L min^{-1}. The Nafion drying system, FROI and LI-COR are shown at the lower portion of the figure. Switching valves directed the flow through or around the Nafion dryer. MFCs 5 and 6 controlled the flow to the FROI and LI-COR and were set at 1.5 L min^{-1}. All data were collected on the data acquisition computer housed in the FROI.

AMTD
6, 9263–9295, 2013

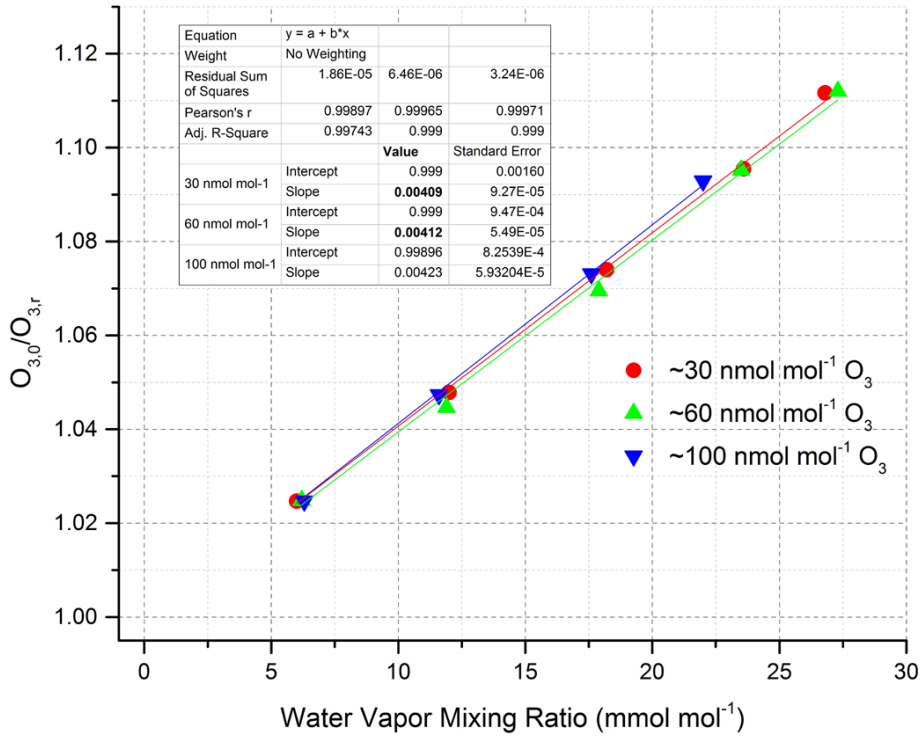

Fig. 3. Ratio of ozone signal at water vapor level less than 0.1 mmol mol^{-1} ($O_{3,0}$) to ozone signal at water vapor level r ($O_{3,r}$) vs. water vapor mole fraction. The points are color-coded by the amount of ozone generated by the TEI 49i. The solid lines represent results from linear regression analyses. The slope results from the linear regression analyses are shown in the table insert.

AMTD
6, 9263–9295, 2013

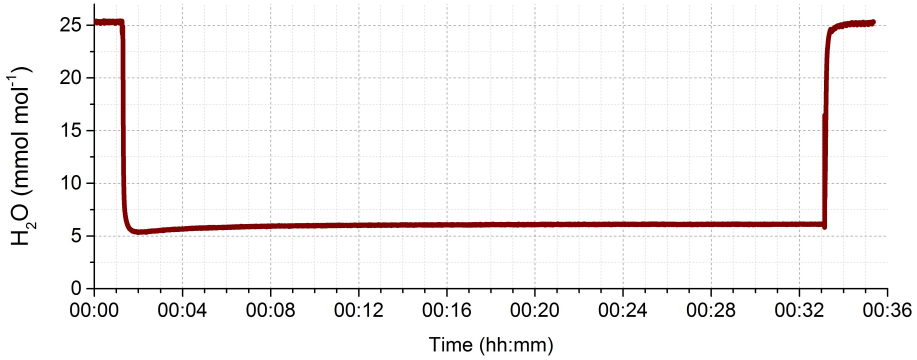

Fig. 4. The water vapor signal before, during and after switching the Nafion dryer into the sample flow.

AMTD
6, 9263–9295, 2013

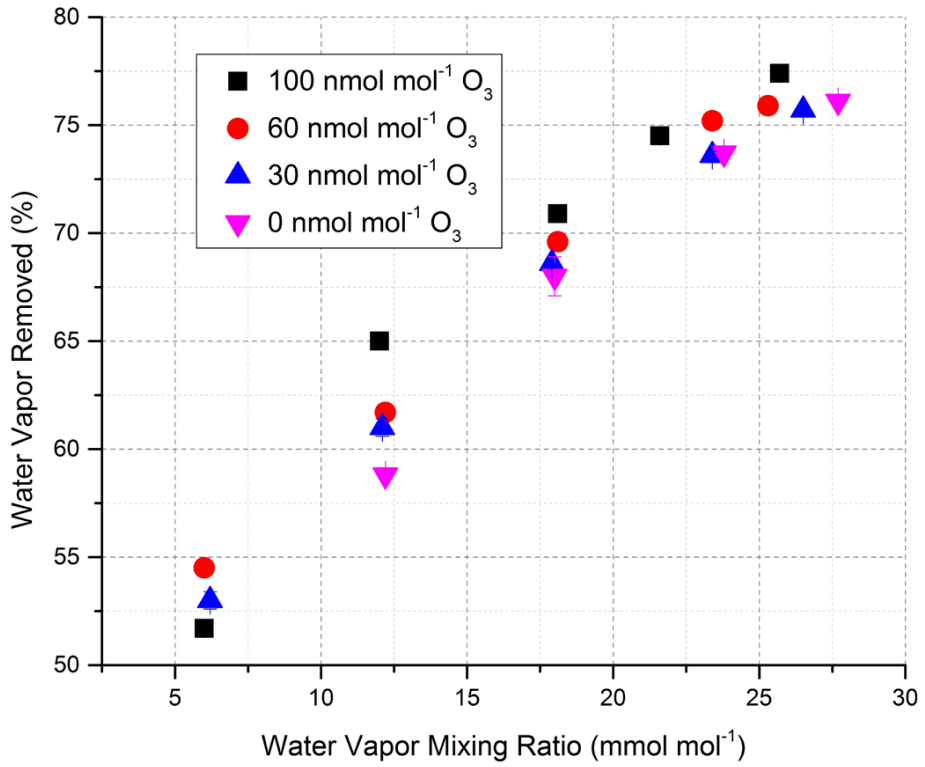

Fig. 5. Fraction of water vapor removed by the Nafion dryer vs. water vapor mole fraction upstream from the Nafion dryer. Data are color-coded by ozone level.

AMTD
6, 9263–9295, 2013

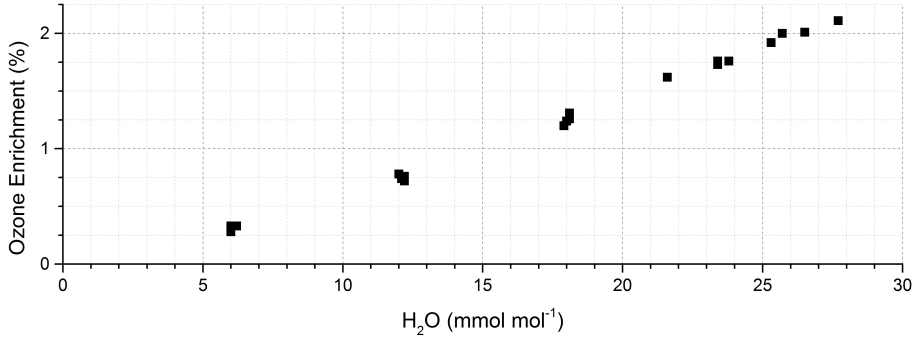

Fig. 6. Increase in the ozone signal from the removal of water vapor molecules by the Nafion dryer as a function of the water vapor mole fraction in the sample air, using the drying efficiency ratios shown in Fig. 5.

AMTD
6, 9263–9295, 2013

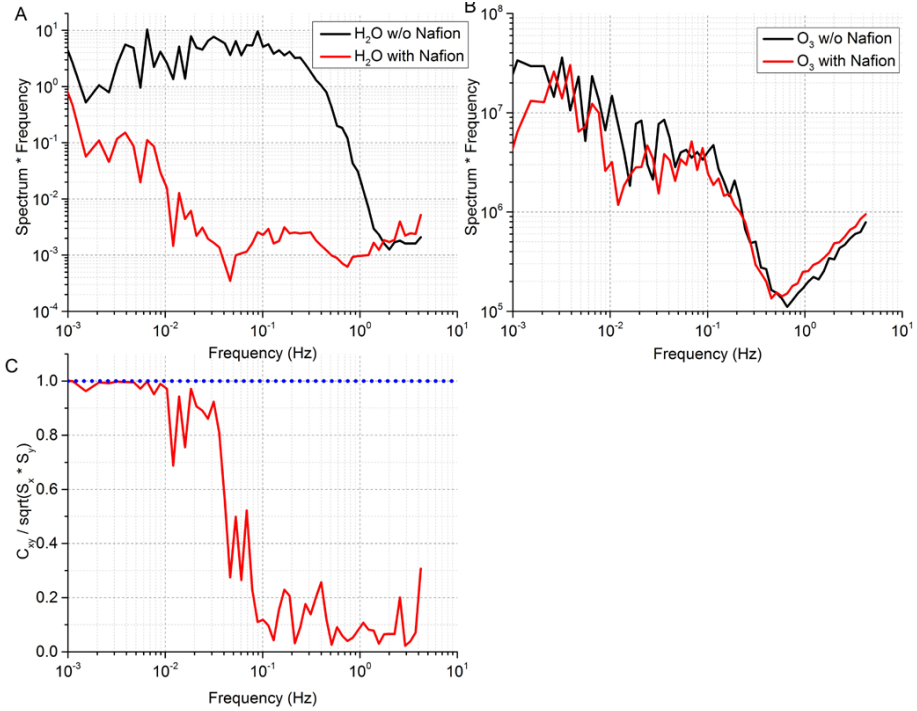

Fig. 7. Spectral distribution plots using two hours of data with the same x-axis range for all three plots. **(A)** Power spectra of ambient water vapor with (red) and without (black) the Nafion drying system. **(B)** Power spectra of the ozone signal with (red) and without (black) the Nafion drying system. **(C)** Coherence spectral distribution of the ambient water vapor signal.

AMTD
6, 9263–9295, 2013

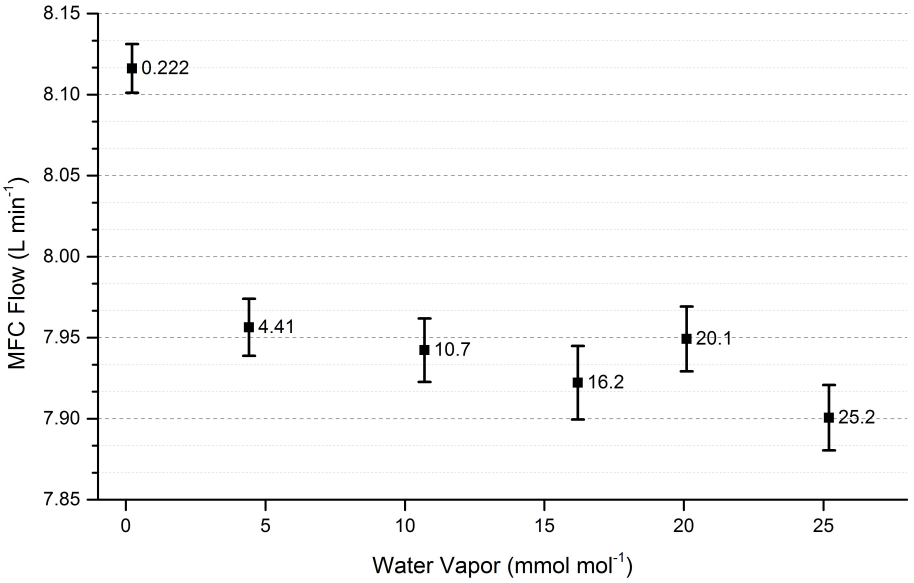

Fig. A1. Flow rate determined with a bubble meter, corrected for ambient pressure and temperature, against water vapor mole fraction, for MFC 3 (Tylan FC-2900) operated at a constant set point. Each point shows the mean flow rate and the error bars represent the standard error with a sample size of 20. The numbers to the right of each point correspond to the water vapor content determined with the LICOR.

AMTD
6, 9263–9295, 2013

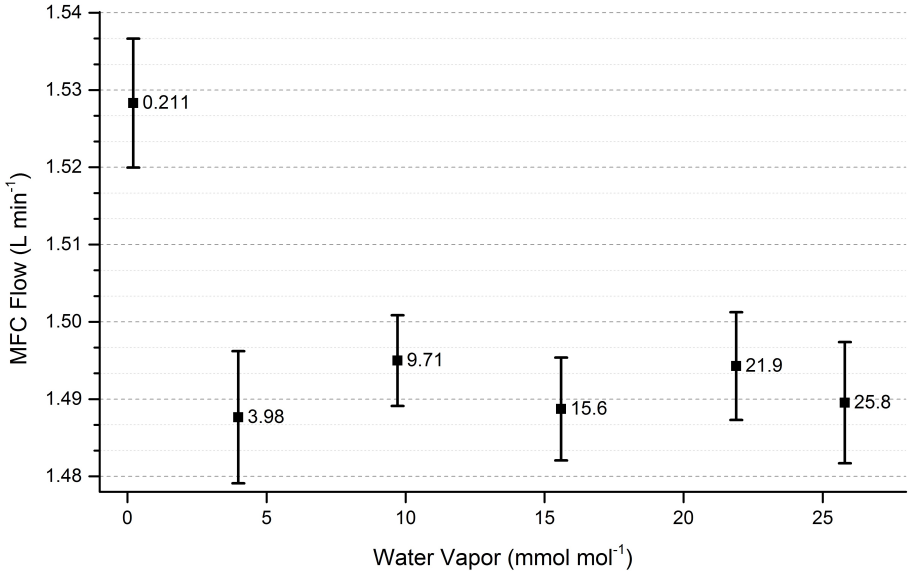

Fig. A2. Flow rate determined with bubble meter, corrected for ambient pressure and temperature, against water vapor mole fraction, for MFC 5 (Tylan FC-260) operated at a constant set point. Each point shows the mean flow rate and the error bars represent the standard error with a sample size of 20. The numbers to the right of each point correspond to the water vapor content determined with the LICOR.

AMTD
6, 9263–9295, 2013